B-mode-guided vector-A-mode versus A-mode biometry to determine axial length and intraocular lens power

Olivier Bergès, MD, Michel Puech, MD, Michael Assouline, MD, PhD, Luc Letenneur, PhD, Marc Gastellu-Etchegorry, MD

ABSTRACT

Purpose: To compare prospectively the reproducibility and accuracy of B-mode-guided biometry with those of A-scan biometry using a conventional A-mode probe to calculate intraocular lens (IOL) power.

Setting: Department of Ophthalmology, Hôtel-Dieu de Paris, France.

Methods: The axial length (AL) in 87 eyes of 72 candidates for cataract surgery was determined by B-mode-guided vector-A-mode and A-mode biometry using an Ophthascan S Ultrasound imager. Patients were assigned to one of two groups based on the B-mode biometry: nonmyopic (AL < 24.5 mm; n = 54) or myopic (AL > 24.5 mm; n = 33). Postoperative refractive results were compared with attempted values.

Results: Mean AL variance was significantly greater when using the A-mode than the B-mode: 0.157 mm ± 0.260 (SD) versus 0.015 ± 0.018 mm in the myopic group ($P < .0001$) and 0.024 ± 0.045 versus 0.009 ± 0.011 mm in the nonmyopic group ($P < .0001$). More eyes having B-mode biometry achieved a final refraction within ±0.50 diopter (D) of the attempted refraction (63 and 43%, respectively; $P < .05$). No deviation greater than 1.60 D was observed with the B-mode in the myopic or nonmyopic group. Three cases with a such a deviation (up to 2.24 D) would have been observed had A-mode-based biometry been chosen for the IOL power calculation. In the myopic group, attempted postoperative refraction was within ±0.50 D in 78% of eyes having B-mode biometry compared with 65% having A-mode. This difference was not statistically significant.

Conclusion: These results suggest that the reproducibility and accuracy of AL measurements are significantly better with B-mode-guided A-mode biometry than with A-mode biometry in myopic and nonmyopic eyes. *J Cataract Refract Surg 1998; 24:529–535*

Preoperative calculation of intraocular lens (IOL) refractive power is based on a number of mathematical formulas.[1–4] These methods are usually derived from regression statistics applied to the postoperative refractive outcome of cataract surgery.[4,5] In addition, some calculation techniques were developed from theoretical models of the eye's optics.[3] Most formulas depend on precise determination of the average preoperative keratometry and axial length (AL) of the eye.[6] Some formulas, therefore, require additional information on anterior chamber depth (ACD) and the central thickness of the crystalline lens.[7]

Reprint requests to Olivier Bergès, MD, Department of Medical Imaging, Fondation Ophtalmologique A. de Rothshild, 29 Rue Manin, 75019 Paris, France.

Although the different mathematical approaches have been extensively described and compared,[8] methods to improve the accuracy of primary keratometry and AL data are seldom discussed.[9–12] Recently, computerized-videokeratography-derived curvature values were shown to be either slightly less accurate[13] or more accurate[14] than standard keratometry values in predicting IOL power.

Conventional AL determination by A-mode ultrasonography is widely accepted as the method of choice for IOL calculation.[6,15] The measure is obtained through subjective alignment of the probe with the visual axis. This alignment relies on obtaining the greatest AL value and the highest amplitude of ultrasound peaks, indicating successive intraocular interfaces of interest. Adequate identification of the front surface of the cornea, anterior and posterior lens capsules, and macular vitreoretinal interface is of critical importance for precise AL measurements by A-mode biometry.

However, correct identification of these landmarks can be difficult in some clinical situations.[9] Depression of the corneal surface from the pressure exerted by the probe in the A-scan contact mode may result in underestimated AL and ACD values. Difficult recognition of the posterior lens surface in eyes with cataract or vitreous-related ultrasonic signals is another potential limitation of A-mode biometry.

The presence of a myopic staphyloma may be the most frequent condition in which precise AL calculation may not be obtained. An oblique rather than orthogonal interception of the ultrasound beam by vitreoretinal interface results from the spatial orientation of the posterior pole surface in myopic staphyloma.[16] This causes a saw-toothed aspect of the peak, which precludes precise localization of the foveolar area. In addition, the steep changes in retinal slope around the macula in high myopia may generate significant AL differences within a small area.

Improved accuracy of the A-scan mode may be achieved by M-mode scanning, in which the external alignment of the transducer probe is video controlled.[17] However, this equipment is not widely available. To our knowledge, the accuracy of the conventional A-scan mode in myopia has not been the subject of a published prospective investigation.

To overcome these limitations, we have used since 1989 a two-dimensional scanning mode (B-scan) to guide the alignment and interpretation of axial biometry in A-scan mode (O. Bergès, "B-Mode Biometry; Indications and Results," presented at the 13th meeting of the International Society for Diagnostic Ophthalmic Ultrasound (SIDUO), Vienna, Austria, July 1990).

We designed a prospective trial to compare the reproducibility and accuracy of a frozen B-mode-based vector-A-mode approach versus a transient-time measurement device using a contact biometry transducer without fixation light scan for axial biometry in myopic and nonmyopic eyes.

Patients and Methods

This prospective study comprised 87 eyes of 72 candidates for cataract surgery. All patients provided informed consent.

The AL of each eye was determined preoperatively by A-mode and B-mode-guided vector-A-mode biometry using an Ophthascan S Ultrasound imager (Alcon-Biophysic Medical). Five measurements were obtained in each eye with no pupil dilation. An AL value obtained at least three times was used to calculate the power of the IOL to be implanted.

Patients were divided into two groups based on the B-scan mode biometry: nonmyopic (AL $<$ 24.5 mm; n = 54) or myopic (AL $>$ 24.5 mm; n = 33) groups. The postoperative refractive results in each group were compared with the attempted values.

A-scan Ultrasound Biometry

Axial length measurements were obtained using topical anesthesia (oxybuprocaine 0.4%) with the patient in a reclining position. Patients were instructed to aim at a colored target attached to the ceiling using binocular fixation. A-mode biometry was performed using a transducer without a built-in fixation light. The probe was gently brought orthogonally to the eye surface until contact with proper peak detection was obtained. The transducer was taken away and contacted again for each of the five measurements. The gates (trigger points) were manually set at a fixed amplitude level.

B-mode-Guided Vector-A-mode Biometry

B-mode biometry was obtained using the same device but with a different probe. A simplified immer-

sion bath was created using the manually opened eyelid fissure filled with carboxymethylcellulose 1% gel (Refractosol®). The probe's tip was held in suspension within the gel layer and without contacting the corneal surface. An optimal axial section of the eye was obtained and a control vector, seen on the screen as a superimposed line, was aligned with the visual axis on the frozen image. An A-scan biometry consisting of four highlighted spots representing intraocular interfaces was reconstructed along the control vector line. Five repeated measurements were obtained from five different B-mode planes in each eye.

Adequacy of the measurement method was ascertained by visualization of dual anterior and posterior corneal interfaces; visualization of the anterior lens surface despite gain attenuation, ascertaining that the control vector was within the pupillary area; alignment of the posterior lens surface with the corneal and anterior lens landmarks; visualization of the widest posterior lens surface; visualization of the vitreoretinal interface in a location temporal to the optic nerve head canal (Figure 1); alignment of the control vector on the four principal landmarks; final alignment of the control vector on the presumed location of the foveola, 15 de-

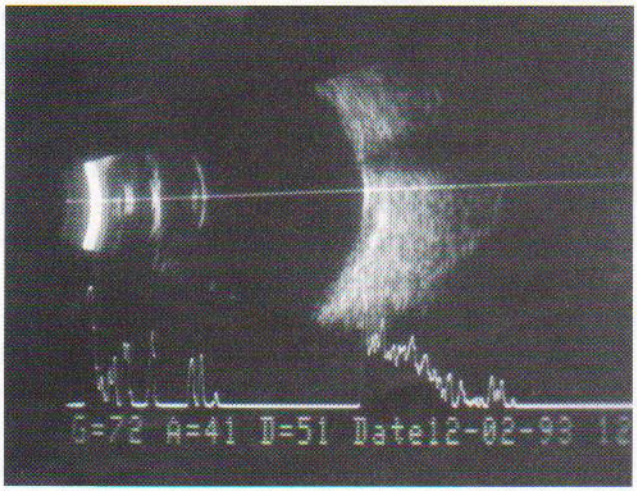

A

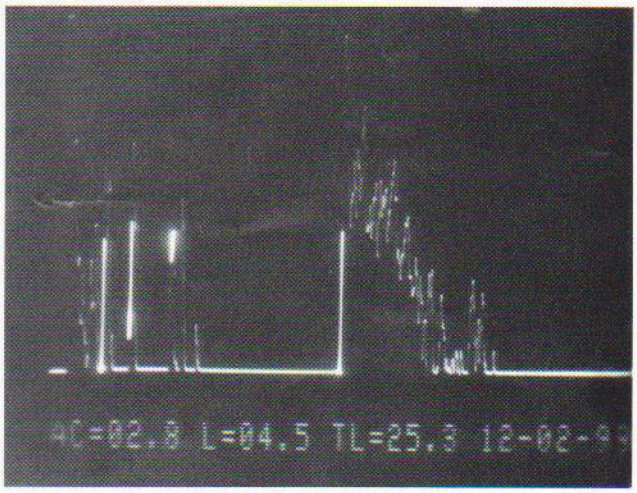

B

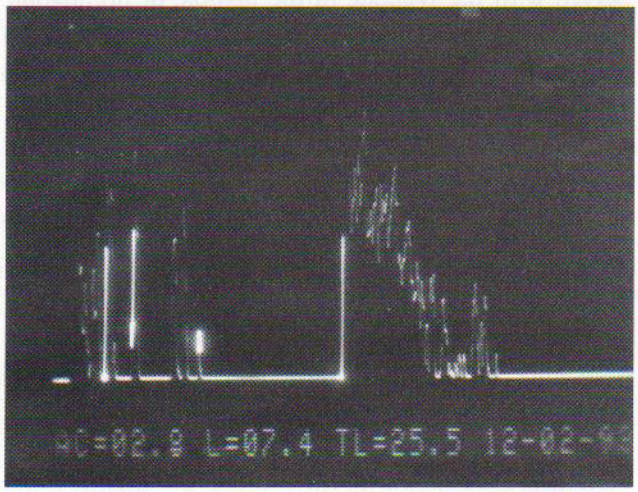

C

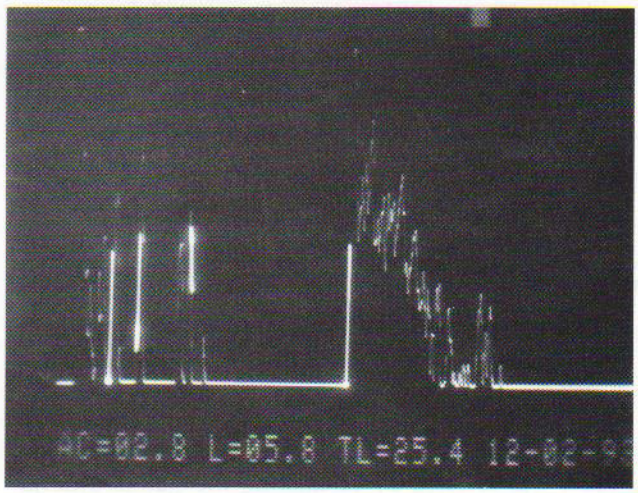

D

Figure 1. (Bergès) *A:* Visualization of the vitreoretinal interface in a location temporal to the optic nerve head canal in B-scan mode with final alignment of the control vector on the presumed location of the foveola, 15 degrees temporally from the optic nerve axis in B-scan mode and correct identification of the posterior lens surface. *B:* The first noncorneal peak of the A-scan is within the crystalline lens. *C:* The third noncorneal peak of the A-scan is within the anterior vitreous. *D:* The second noncorneal peak of the A-scan corresponds to the posterior crystalloid as demonstrated by the B-scan.

grees temporally from the optic nerve axis (Figure 1). This geometrical approach of the foveolar location is an estimate that can be limited in application because the axial sector-scan B-mode presentation of the eye may be distorted by sound refraction.

Calculation of axial biometry was performed by adding the distances between intraocular landmarks using specific sound-propagation speeds for each intraocular segment (anterior chamber 1532 ms, lens 1641 ms, vitreous 1532 ms). This method seems more precise than simply averaging the ultrasound velocities in the various intraocular media.[18]

All measurements were obtained within 10 minutes of the first A-mode measurement to limit potential changes in choroidal thickness from repeated pressure applications on the eye.

Lens Calculation, Surgery, Follow-up

In all eyes, IOL power was calculated using the SRK/T formula and the appropriate A-constant. Surgery was performed by phacoemulsification by nine surgeons in all cases but six, in which manual extracapsular extraction was indicated.

Three months postoperatively, combined spherical and cylindrical refraction was determined subjectively based on the red/green test to evaluate stability of results. Refraction could be determined in 51 eyes, 23 myopic and 28 nonmyopic. Appropriate refraction could not be obtained in 4 eyes because of visual acuity less than 20/200. An additional 18 patients were lost to follow-up at 3 months.

Analysis of attempted versus achieved refraction was done on the basis of the ultrasonic biometry before surgery; thus, the achieved IOL position with its influence on refraction and actual retinal position, depending also on choroidal thickness after IOL implantation, was not considered in the analysis.

Statistical Analysis

The reproducibility of the two biometry techniques was assessed by calculating the standard deviation and variance of the five measurements obtained for each eye with each of the two methods. Comparison of mean values for the variance and standard deviation of the measurements between myopic and nonmyopic groups and A-mode versus B-mode was done using a nonparametric Mann–Whitney test. Clinical accuracy of the method was analyzed by comparing attempted with achieved postoperative refraction (spherical equivalent).

Postoperative refractive results were evaluated at 3 months in 51 eyes. The comparison of the difference between refractive deviation (difference between attempted and achieved postoperative refraction) as a function of biometry mode was performed using a Student's *t*-test and chi-square test.

Results

Mean AL variance was significantly greater using the A-mode than the B-mode (Table 1): 0.157 ± 0.260 versus 0.015 ± 0.018 mm in the myopic group and 0.024 ± 0.045 versus 0.009 ± 0.011 mm in the nonmyopic group ($P < .0001$). This suggests that the reproducibility of AL measurement was significantly better with the B-scan than the A-scan mode in both myopic and nonmyopic eyes, with the reproducibility more pronounced in the myopic group.

In the overall population, a significantly larger proportion of eyes with B-mode-based biometry achieved a final refraction within ±0.50 diopter (D) of attempted correction than eyes with A-mode-based biometry (63 versus 43%; $P < .05$) (Table 2). In addition, no deviation greater than 1.60 D was observed with the B-mode in the myopic or nonmyopic group. Three cases of such a deviation (up to 2.24 D) would have been observed had the A-mode-based biometry been used to calculate IOL power (Figures 2 and 3). In the myopic group, accuracy of the attempted postoperative refraction was achieved within ±0.50 D in 78% of eyes with the B-mode and 65% with the A-mode. This difference was not statistically significant in this myopic or nonmyopic group.

Mean refractive deviation (the absolute value of the difference between attempted and achieved spherical equivalent) was not significantly affected by the biometric mode. In 51 eyes at 3 months, mean refractive deviation associated with the B-mode was slightly lower than with the A-mode (0.69 ± 0.53 versus 0.52 ± 0.48 D), but the difference was not statistically significant.

A-mode and B-mode guided vector-A-mode biometry had an equal tendency to underestimate (10, both

Table 1. Variance in AL measurements, A-scan versus B-scan mode.

Group	Axial Length (mm)				
	A-scan	B-scan	B > A	A > B	A = B
Total					
n	51.00	51.00	23.00	11.00	17.00
Mean	0.69	0.52	0.59	0.44	0.00
SD	0.53	0.48	0.47	0.26	0.00
Min	0.00	0.00	0.08	0.22	0.00
Max	2.24	1.59	1.71	1.13	0.00
Myopic					
n	23.00	23.00	11.00	5.00	7.00
Mean ± SD	0.70	0.50	0.64	0.49	0.00
SD	0.59	0.42	0.53	0.37	0.00
Min	0.01	0.01	0.08	0.24	0.00
Max	2.24	1.56	1.67	1.13	0.00
Nonmyopic					
n	28.00	28.00	12.00	6.00	10.00
Mean ± SD	0.67	0.53	0.54	0.41	0.00
SD	0.48	0.51	0.44	0.16	0.00
Min	0.00	0.00	0.15	0.22	0.00
Max	1.98	1.59	1.71	0.63	0.00

Min = minimum; Max = maximum; n = number of eyes

methods) or overestimate (13, both methods) AL in myopic eyes. However, both A- and B-scan biometry modes led to a much higher proportion of overestimated ALs in nonmyopic eyes (23 and 19, respectively) than underestimated measurements (5 and 9, respectively). This trend resulted in a shift of refractive deviation toward residual hyperopia.

Discussion

The potential benefits of B- mode over A-mode biometry may include the ability to precisely identify the visual axis on an axial bidimensional ultrasonic section of the eye. In addition, simplified immersion techniques allow preservation of the actual ACD by

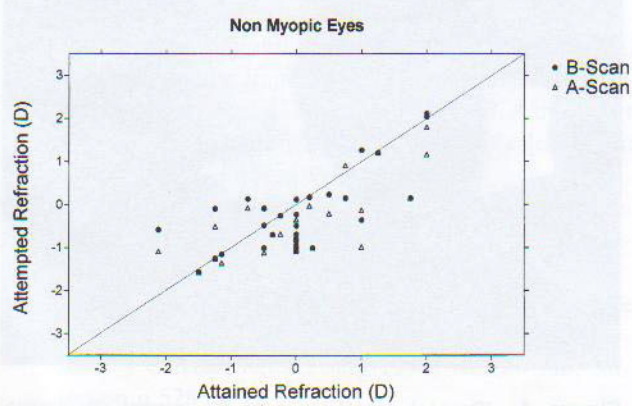

Figure 2. (Bergès) Attempted versus attained postoperative refraction in nonmyopic eyes for A-scan and B-scan mode.

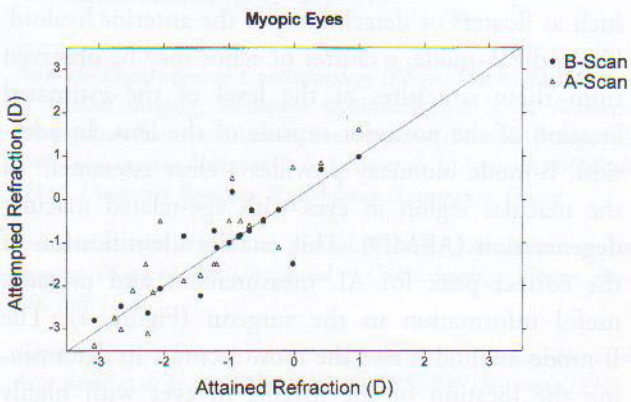

Figure 3. (Bergès) Attempted versus attained postoperative refraction in myopic eyes for A-scan and B-scan mode

Table 2. Postoperative refractive results at 3 months in 51 eyes. Comparison of the algebraic and absolute differences between attempted and achieved postoperative refraction as a function of biometry mode.

	A-Mode		B-Mode			
Group	**Algebraic**	**Absolute**	**Algebraic**	**Absolute**	**DSA**	**DSB**
Myopic						
Mean	0.296	0.703	0.202	0.503	0.301	0.102
SD	0.880	0.592	0.630	0.419	0.260	0.071
Max	2.240	2.240	1.560	1.560	0.996	0.259
Min	−1.030	0.010	−0.860	0.010	0.045	0.000
n	23.000	23.000	23.000	23.000	33.000	33.000
Nonmyopic						
Mean	0.458	0.674	0.202	0.530	0.131	0.080
SD	0.693	0.477	0.717	0.514	0.086	0.050
Max	1.980	1.980	1.590	1.590	0.540	0.230
Min	−1.030	0.000	−1.540	0.000	0.000	0.000
n	28.000	28.000	28.000	28.000	58.000	58.000

DSA = standard deviation for the A-mode; DSB = standard deviation for the B-mode; Min = minimum; Max = maximum; n = number of eyes

preventing corneal indentation induced by the ultrasonic probe.

B-scans also provide for improved discrimination between peaks associated with the anterior lens surface and those associated with the iris, a distinction made difficult when the ultrasonic beam is not properly aligned with the center of the pupillary area as in the A-scan mode. When the B-mode is used, the distinction between the posterior lens surface and echogenic surfaces and artifacts within the cataractous crystalline lens is much clearer than with the A-mode. This permits more accurate positioning of the measuring spot along the posterior lens capsule.

This is also true for anterior intravitreal structures such as floaters or detachment of the anterior hyaloid. Using the A-mode, a cluster of echos may be observed from these structures at the level of the estimated location of the posterior capsule of the lens. In addition, B-mode biometry provides a clear assessment of the macular region in eyes with age-related macular degeneration (ARMD). This enables identification of the correct peak for AL measurement and provides useful information to the surgeon (Figure 4). The B-mode method is also the most accurate in determining the location of the foveola in eyes with highly myopic globes and significant deformation of the posterior pole from staphyloma. However, in eyes with major ectatic changes in the posterior sclera, the oblique orientation of the macular plane with respect to the direction of the ultrasonic beam is still responsible for large variations in the measurements that cannot be fully resolved.[16,19]

These results suggest that B-mode biometry is more reproducible and reduces the risk of significant refractive errors in IOL power calculation. Other parameters, such as the effective diameter and homogeneity of the sound field at the lens and retinal position,[12] or the electronic features of the equipment, including

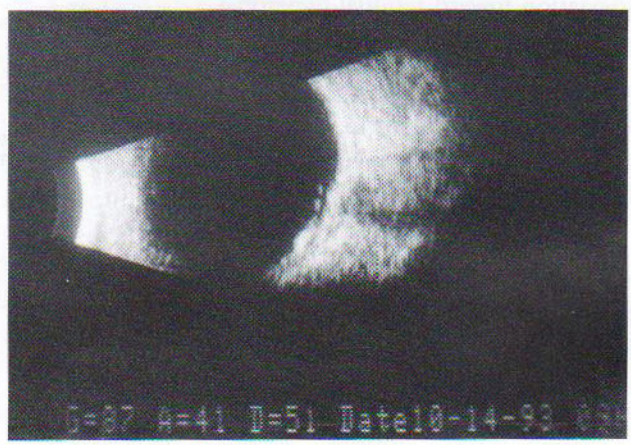

Figure 4. (Bergès) Identification of the correct vitreoretinal peak for axial length measurement in an eye with ARMD in B-scan mode.

the axial and lateral pixel resolution of digital memories and displays, are independent of the operating mode A or B and may greatly influence the distance measured and the reproducibility during biometry. In this study, a single device, with identical electronic features, including resolution of digital memory and display, was used for both A- and B-modes. However, the transducers used in this comparative study were different for each mode, and the differences in performance parameters between these transducers may have contributed in part to the differences observed in the refraction results. Numerous other commercial B- and A-mode systems with lower or higher level of performance are available, and the results of this study might be equipment dependent.

In our study, conclusions about underestimation or overestimation of AL were based on calculations using achieved postoperative refractions, preoperative AL and AC values, and a specific IOL formula characterized by its specific errors. Thus, the refractive results do not necessarily provide evidence of superiority of B-mode biometry because the true AL of the patients was not known. Rather, the refractive results reflect that specific errors associated with this B-mode technique fit better with the errors associated with the SRK/T formula than the specific errors resulting from the A-mode used in this study.

Additional investigation of myopic eyes with B-mode is warranted to further demonstrate the benefit of this method for the improvement of the refractive predictability of cataract surgery with IOL implantation.

References

1. Binkhorst RD. IOL power calculation. Int Ophthalmol Clin 1979; 19(4):237–252
2. Retzlaff J. A new intraocular lens calculation formula. Am Intra-Ocular Implant Soc J 1980; 6:148–152
3. Holladay JT, Prager TC, Chandler TY, et al. A three-part system for refining intraocular lens power calculations. J Cataract Refract Surg 1988; 14:17–24
4. Sanders DR, Retzlaff JA, Kraff MC, et al. Comparison of the SRK/T formula and other theoretical and regression formulas. J Cat Refract Surg 1990; 16:341–346
5. Retzlaff JA, Sanders DR, Kraff MC. Development of the SRK/T intraocular lens implant power calculation formula. J Cataract Refract Surg 1990; 16:333–340; correction p 528
6. Butcher JM, O'Brien C. The reproducibility of biometry and keratometry measurements. Eye 1991; 5:708–711
7. Olsen T. Sources of error in intraocular lens power calculation. J Cataract Refract Surg 1992; 18:125–129
8. Olsen T, Thim K, Corydon L. Theoretical versus SRK I and SRK II calculation of intraocular lens power. J Cataract Refract Surg 1990; 16:217–225
9. Giers U, Epple C. Comparison of A-scan device accuracy. J Cataract Refract Surg 1990; 16:235–242
10. Uchihori Y, Emi K, Tsuboi S. The accuracy of ocular biometry by B-mode echography. Acta Soc Ophthalmol Jpn 1983; 87:398–402
11. Olsen T, Nielsen PJ. Immersion versus contact technique in the measurement of axial length by ultrasound. Acta Ophthalmol 1989; 67:101–102
12. Husain SE, Kohnen T, Maturi R, et al. Computerized videokeratography and keratometry in determining intraocular lens calculations. J Cataract Refract Surg 1996; 22:362–366
13. Assouline M, Briat B, Kaplan-Messas A, et al. Analyse videokératoscopique informatisée et chirurgie de la cataracte par phacoemulsification. Calcul prédictif de la puissance de l'implant intraoculaire. J Fr Ophtalmol 1997; 20:411–417
14. Hoffer KJ. Preoperative evaluation of the cataractous patient. Surv Ophthalmol 1984; 29:55–69
15. Curtin BJ. The natural history of posterior staphyloma development. Doc Ophthalmol Proc Ser 1981; 28:207–213
16. Jensen PK, Rask R, Olsen T. Video controlled M-mode biometry. Acta Ophthalmol Scand 1995; 73:61–65
17. Hoffer KJ. Ultrasound velocities for axial eye length measurement. J Cataract Refract Surg 1994; 20:554–562
18. Fernandez-Vigo J, Castro J, Diaz J, Cid MR. Ultrasonic forms of posterior staphyloma. Ann Ophthalmol 1990; 22:391–394
19. Eisenberg A, Kütnicke E, Lötsche R, et al. Measurement and computer simulation of ultrasonic fields of medical A-mode transducers regarding diagnostic performance. Proceedings of the World Congress on Ultrasonics. Berlin, Elsevier, 1995; 915–918

From the Department of Ophthalmology (Bergès, Puech), Department of Medical Imaging, Fondation Ophtalmologique A. de Rothshild (Bergès, Assouline), and Médecins Sans Frontières (Gastellu-Etchegorry), Paris, and Institut National de la Santé et de la Recherche Médicale U330, Université Bordeaux II, Bordeaux (Letenneur), France.

Presented in part at the 13th Annual Meeting of the Symposium on Imaging Diagnosis and Ultrasound in Ophthalmology, Vienna, Austria, July 1990.

Supported in part from an unrestricted grant from the Institut National de la Santé et de la Recherche Médicale (INSERM U86 and U330).

None of the author has a financial interest in any device or product mentioned.